LETTER

doi:10.1038/nature14679

Conformational dynamics of a class C G-protein-coupled receptor

Reza Vafabakhsh[1]*, Joshua Levitz[1]* & Ehud Y. Isacoff[1,2,3]

G-protein-coupled receptors (GPCRs) constitute the largest family of membrane receptors in eukaryotes. Crystal structures have provided insight into GPCR interactions with ligands and G proteins[1,2], but our understanding of the conformational dynamics of activation is incomplete. Metabotropic glutamate receptors (mGluRs) are dimeric class C GPCRs that modulate neuronal excitability, synaptic plasticity, and serve as drug targets for neurological disorders[3,4]. A 'clamshell' ligand-binding domain (LBD), which contains the ligand-binding site, is coupled to the transmembrane domain via a cysteine-rich domain, and LBD closure seems to be the first step in activation[5,6]. Crystal structures of isolated mGluR LBD dimers led to the suggestion that activation also involves a reorientation of the dimer interface from a 'relaxed' to an 'active' state[7,8], but the relationship between ligand binding, LBD closure and dimer interface rearrangement in activation remains unclear. Here we use single-molecule fluorescence resonance energy transfer to probe the activation mechanism of full-length mammalian group II mGluRs. We show that the LBDs interconvert between three conformations: resting, activated and a short-lived intermediate state. Orthosteric agonists induce transitions between these conformational states, with efficacy determined by occupancy of the active conformation. Unlike mGluR2, mGluR3 displays basal dynamics, which are Ca^{2+}-dependent and lead to basal protein activation. Our results support a general mechanism for the activation of mGluRs in which agonist binding induces closure of the LBDs, followed by dimer interface reorientation. Our experimental strategy should be widely applicable to study conformational dynamics in GPCRs and other membrane proteins.

Single-molecule fluorescence resonance energy transfer (smFRET) spectroscopy is a powerful tool for high-resolution probing of protein conformational change[9], and was recently applied to study membrane proteins[10–12]. To visualize ligand-induced rearrangements of full-length mGluRs, we used previously described amino-terminal SNAP- or CLIP-tagged proteins (Fig. 1a), permitting the selective and orthogonal introduction of either a FRET donor or an acceptor fluorophore into each subunit of the dimer, near the LBD[13,14]. Electrophysiological recordings in cells co-expressing the G-protein-gated inward rectifier potassium channel (GIRK) showed that these constructs were physiologically functional (Extended Data Fig. 1a). SNAP–mGluR2 and CLIP–mGluR2 were expressed in HEK293T cells and labelled with FRET donor (DY-547) and acceptor (Alexa-647) fluorophores, respectively (Methods and Extended Data Fig. 1b). Glutamate induced a concentration-dependent decrease in ensemble FRET (Extended Data Fig. 1c, d), as previously shown[15]. For the smFRET assay, we used single-molecule pull-down[16] with an anti-carboxy-terminal antibody for *in situ* immunopurification of labelled receptors from HEK293T cell lysate, followed by total internal reflection fluorescence microscopy (Fig. 1b and Extended Data Fig. 2a). The pull-down was specific, mGluR2 remained a dimer after pull-down (Extended Data Fig. 2b, c), and there was no cross labelling between the SNAP and CLIP tags (Extended Data Fig. 2d).

In the absence of glutamate, the smFRET efficiency was ~0.45 (Fig. 1c, top), and saturating glutamate (1 mM) shifted this to ~0.2 (Fig. 1c, bottom), consistent with ensemble FRET (Extended Data Fig. 1c). Both the 0 and 1 mM glutamate states were stable within our time resolution (30 ms), with few transitions to other FRET levels. However, at intermediate glutamate concentrations, mGluR2 displayed rapid transitions between three distinct states: the 0.45 (high) FRET level seen in 0 mM glutamate, the 0.2 (low) FRET level seen in 1 mM glutamate, and a short-lived 0.35 (medium) FRET level (Fig. 1d, e and Extended Data Fig. 3a). The competitive antagonist LY341495 produced a similar FRET histogram to that seen in 0 mM glutamate: a major high FRET peak (0.45) and a minor medium FRET peak (~0.35) (Fig. 1e, bottom). About 20% of individual FRET trajectories showed visits to the low FRET state in 0 mM glutamate (Extended Data Fig. 3b), but these transitions were rare and brief and, thus, almost undetectable in the FRET histograms (Fig. 1e, top). Control experiments with an antibody against the mGluR2 N terminus instead of the C terminus showed identical histograms (Extended Data Fig. 2e, f). Moreover, the application of GTP or apyrase, to favour receptor association or dissociation from G proteins, respectively, did not alter the smFRET histograms (Extended Data Fig. 2g), indicating that G proteins are not co-immunoprecipitated with mGluR2.

Because mGluR2 did not induce G-protein signalling in the presence of 0 mM glutamate or LY341495 (Extended Data Fig. 3c), we proposed that the high and medium FRET states represent functionally inactive conformations, and that the low FRET state corresponds to the active state. Consistent with this interpretation, the low FRET state glutamate concentration-dependence had a half-maximum effective concentration (EC_{50}) value of 5.7 ± 0.3 μM (mean ± s.e.m.) (Fig. 1f and Extended Data Fig. 3d), corresponding to the concentration-dependence of GIRK current activation in HEK293T cells (3.2 ± 0.3 μM) (Extended Data Fig. 3e). Moreover, glutamate had no effect on the FRET histogram in the glutamate-insensitive mutant mGluR2-YADA (Tyr216Ala, Asp295Ala)[17] (Extended Data Fig. 3g). Finally, the addition of LY341495 to glutamate abolished the low FRET state (Extended Data Fig. 3h). These observations confirm the assignment of the low FRET peak to the active conformation.

We next quantified the glutamate-induced fluctuations with cross-correlation and dwell-time analyses. The cross-correlation amplitude of donor and acceptor signals increased with glutamate concentration, reaching a maximum near the EC_{50} value, and decreased at high glutamate concentrations (Fig. 1g). Anti-correlation between donor and acceptor was almost abolished in saturating glutamate (1 mM), confirming the stabilization of the active state. Kinetic analysis of individual traces showed an ~84-ms active state dwell time that was nearly independent of glutamate concentration (Fig. 1h and Extended Data Fig. 3i), suggesting that the active state dwell time reflects the glutamate dissociation rate and the inherent stability of the active

[1]Department of Molecular and Cell Biology, University of California, Berkeley, California 94720, USA. [2]Helen Wills Neuroscience Institute, University of California, Berkeley, California 94720, USA. [3]Physical Bioscience Division, Lawrence Berkeley National Laboratory, Berkeley, California 94720, USA.
*These authors contributed equally to this work.

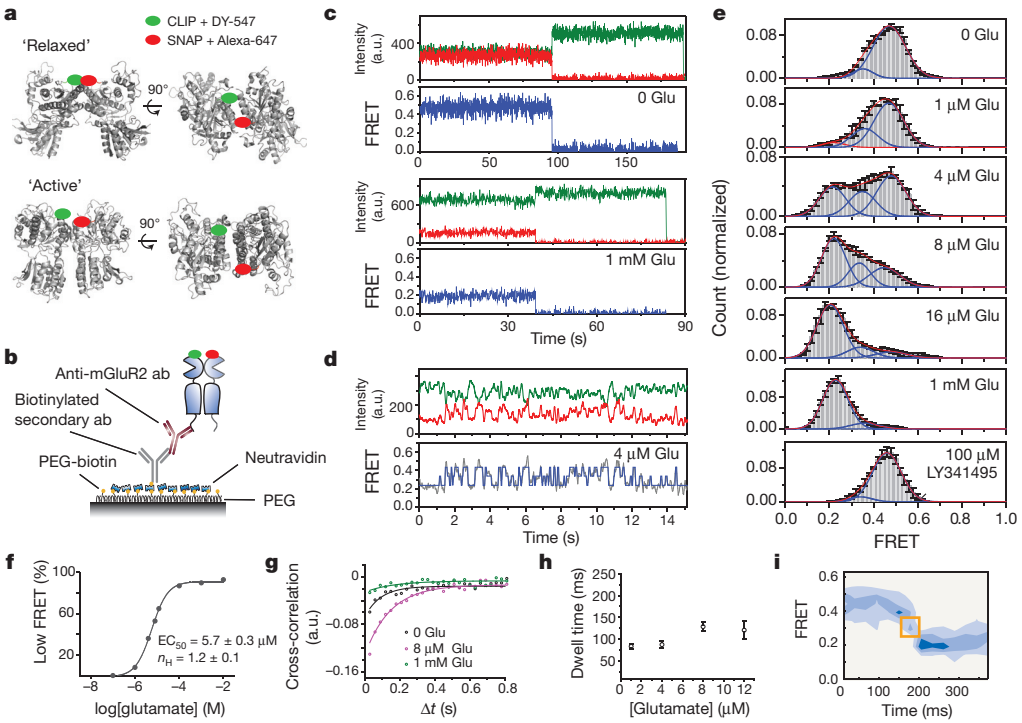

Figure 1 | A single-molecule FRET assay reveals three conformations of the mGluR2 activation pathway. **a**, Crystal structures of mGluR1 in the 'relaxed' (Protein Data Bank (PDB) accession 1EWT) and 'active' states (PDB code IEWK) show an increase in the distance between N termini after activation. Red and green ovals show the approximate positions of SNAP and CLIP tags, respectively. **b**, Schematic of single-molecule FRET measurements. Ab, antibody. **c**, Donor (green) and acceptor (red) intensity time traces and FRET trace (blue) in the absence (top) or presence (bottom) of 1 mM glutamate show a decrease in FRET in the presence of saturating glutamate. a.u., arbitrary units. **d**, Representative smFRET traces at 4 μM glutamate reveal rapid dynamics between three states. A three-state fit obtained from hidden Markov analysis is overlaid over the filtered raw data. **e**, smFRET histograms in the presence of a range of glutamate concentrations or a competitive antagonist (LY341495). Blue lines show global three-component Gaussian fits that show the high (~0.45), medium (~0.35) and low (0.2) FRET states. The sum of all three components is shown in red. **f**, Titration curve for the low FRET peak. n_H, Hill coefficient. **g**, Cross-correlation plots show limited dynamics in the absence of glutamate (black) or in saturating glutamate (1 mM, green), but enhanced dynamics at intermediate concentrations (8 μM, magenta). Solid lines show single exponential fits. **h**, Concentration dependence of low FRET dwell times obtained from dwell time analysis. **i**, FRET density plots constructed from synchronized transitions from the high to low FRET states show a short dwell at the medium FRET level (yellow box). Error bars are s.e.m.

conformation. Two-dimensional histograms obtained from synchronized transitions into or out of the low FRET state showed a short dwell at the medium FRET value of ~0.35, providing additional evidence that this state is an intermediate in the activation pathway (Fig. 1i and Extended Data Fig. 3j).

Next, we investigated the relationship between ligand efficacy and receptor conformation. We studied two group II mGluR agonists, the efficacies of which differ from that of glutamate[15] (Fig. 2a). While DCG-IV increased the occupancy of the low FRET state, even at saturating concentrations (≥100 μM), the low FRET state was not fully occupied and ~30% of the distribution remained in the high and medium FRET states (Fig. 2b). Single-molecule traces in saturating DCG-IV showed recurrent transitions out of the low FRET state (Fig. 2c, d and Extended Data Fig. 4a). By contrast, the full-agonist LY379268 populated the same three FRET states but with more complete occupancy of the active state than glutamate (Fig. 2e and Extended Data Fig. 4b, c). Consistent with these results, cross-correlation analysis showed that mGluR2 retained substantial dynamics in saturating DCG-IV, but not in saturating glutamate or LY379268 (Fig. 2d). Notably, at concentrations that produced comparable occupancy of the low FRET state (Extended Data Fig. 4d), cross-correlation analysis showed that LY379268 induced longer timescale fluctuations and longer active state dwell times than did glutamate and DCG-IV (Fig. 2f–h and Extended Data Fig. 4e, f). Two-dimensional histograms showed that both DCG-IV and LY379268, like glutamate, visit the medium FRET state as an intermediate during activation (Extended Data Fig. 4g, h). Thus, unlike ionotropic receptors, in which the efficacy of an agonist is a function of the degree of LBD closure[18], in mGluR2, agonists with different efficacies stabilize the same conformational states, with the degree of efficacy depending on the occupancy of a single active conformation. The data suggest that ligand efficacy depends more on the rate of transition into the active state than on dwell time in the active state; that is, that agonists differ in how they induce LBD closure and subsequent reorientation. Additionally, an mGluR2-specific positive allosteric modulator, LY48739, and the transmembrane domain (TMD) mutations Gln679Val and Cys770Ala (refs 19, 20), which all increase the efficacy of DCG-IV, also increased the relative occupancy of the low FRET state (Extended Data Fig. 5), further supporting the role of active state occupancy in determining agonist efficacy, and confirming that the immobilized receptors retain TMD function and coupling to the LBD.

We next wondered whether the properties of mGluR2 apply to other mGluRs. We turned to the other group II mGluR, mGluR3, which possesses ~70% sequence identity with mGluR2. SNAP- or CLIP-tagged mGluR3 constructs were physiologically functional (Extended Data Fig. 6a) and underwent a glutamate-dependent decrease in ensemble FRET similar to mGluR2, but with a lower EC_{50} value (0.5 ± 0.2 μM). Notably, single-molecule trajectories of mGluR3 in 0 mM glutamate exhibited frequent transitions between the three FRET states (Fig. 3a, top), resulting in ~30% occupancy of the low FRET active state (Extended Data Fig. 6b, c), which was eliminated by LY341495 (Fig. 3a, bottom; Extended Data Fig. 6b, c). LY341495 produced a large decrease in the glutamate-free GIRK current (Fig. 3b, c and Extended Data Fig. 6d) and ensemble FRET (Extended Data

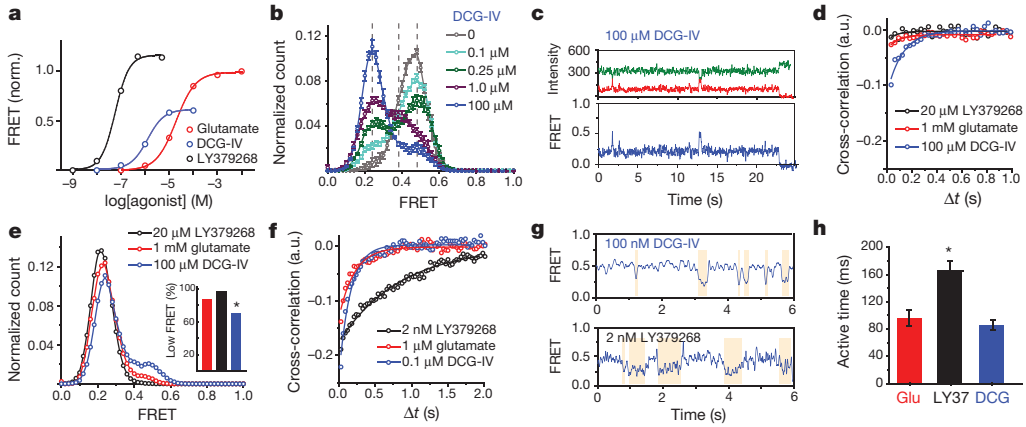

Figure 2 | Conformational basis of partial agonism of mGluR2. **a**, Ensemble FRET titrations in HEK293T cells expressing mGluR2 in the presence of glutamate (red), DCG-IV (blue) or LY379268 (black). FRET values in each condition are normalized to the response to 1 mM glutamate. **b**, smFRET histogram for DCG-IV shows the same three states as seen for glutamate (dotted lines), with dose-dependent occupancy of the low FRET state. **c**, Representative smFRET trace shows transitions out of the low FRET state in saturating DCG-IV. **d**, Cross-correlation plots for saturating agonist reveal dynamics = DCG-IV > glutamate > LY379268. Solid lines show single exponential fits. **e**, smFRET histograms for saturating agonist; occupancy of the low FRET state = DCG-IV < glutamate < LY379268 (inset). $*P = 0.008$, two-tailed *t*-test. **f**, **g**, At concentrations that result in comparable population of the active state, LY379268 induces slower dynamics than DCG-IV and glutamate as shown in cross-correlation and fit to a single exponential function (**f**) and representative smFRET traces (**g**). **h**, LY379268 induces significantly longer low FRET state dwell times than glutamate and DCG-IV (two-tailed *t*-test, $*P = 0.0084$). Error bars are s.e.m.

Fig. 6e, f) in cells expressing mGluR3, but not in cells expressing mGluR2, indicating that, unlike mGluR2, mGluR3 has basal activity. Importantly, the 0 mM glutamate smFRET distribution of mGluR3 was insensitive to GTP, indicating that the different basal activity of mGluR3 is not due to association with G protein (Extended Data Fig. 6g).

Earlier work suggested that some mGluRs, including mGluR3 but not mGluR2, are calcium-sensitive[21]. However, direct binding of Ca^{2+} has been challenged, and Ca^{2+} activity was attributed to indirect downstream signalling effects[22]. smFRET measurements of mGluR3 in 0 mM glutamate and 0 mM Ca^{2+} showed a significant reduction of basal dynamics and occupancy of the low FRET state (Fig. 3d, e and Extended Data Fig. 7a, b). In 0 mM glutamate, we observed a Ca^{2+}-concentration-dependent increase in low FRET state occupancy dynamics (Extended Data Fig. 7c, d). By contrast, removal of Ca^{2+} did not alter the smFRET properties of mGluR2 (Extended Data Fig. 7f, g). Saturating glutamate (0.5 mM) induced the same mGluR3 smFRET histogram in 0 and 2 mM Ca^{2+}, indicating that Ca^{2+} is not required for full agonism of mGluR3 (Fig. 3d, e). Similar to the orthosteric agonists on mGluR2, in mGluR3, Ca^{2+} induced transient occupancy of the intermediate FRET state (Extended Data Fig. 7e). The mutation Ser152Asp, which is reported to abolish the Ca^{2+} sensitivity of both mGluR1 and mGluR3 (ref. 21), eliminated the effect of LY341495 on mGluR3 (Extended Data Fig. 8a–c), indicating elimination of basal activity. Consistent with this, smFRET analysis of mGluR3(Ser152Asp) revealed a large reduction in basal low FRET population and Ca^{2+} sensitivity (Fig. 3d and Extended Data Fig. 8d, e) and a decrease in receptor dynamics (Fig. 3f and Extended Data Fig. 8f). Dwell-time analysis of mGluR3 in the presence of 2 mM Ca^{2+} or 100 nM glutamate (Fig. 3g, h and Extended Data Fig. 9a, b) showed an average active state lifetime of 183 ms, significantly longer than the ~80 ms lifetime in mGluR2 (Fig. 1h), indicating that the

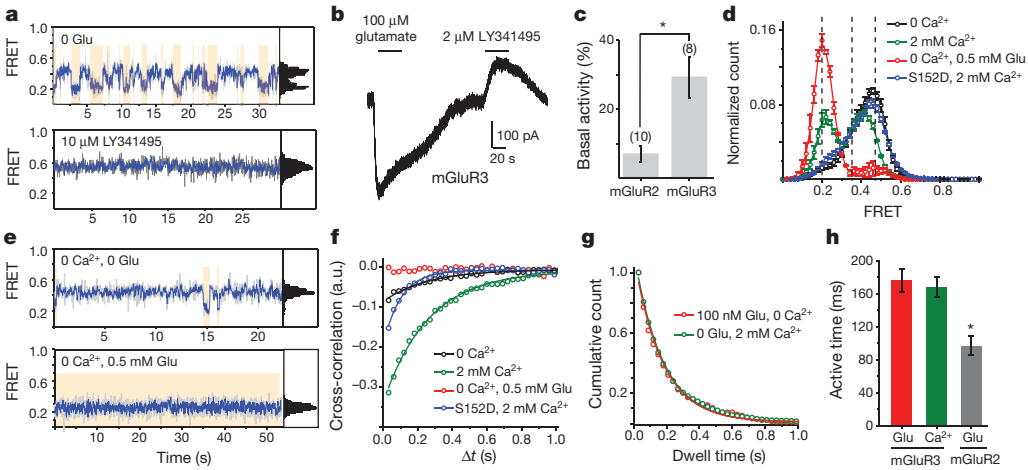

Figure 3 | mGluR3 has high basal structural dynamics and activity. **a**, Representative mGluR3 smFRET traces show basal dynamics in the absence of glutamate (top) that are abolished by the competitive antagonist LY341495 (bottom). **b**, In HEK293T cells co-expressing GIRK channels, mGluR3 has basal activity in the absence of glutamate, which is blocked by LY341495. **c**, Basal activity ($[I_{LY341495}]/([I_{LY341495}] + [I_{Glu}])$) for mGluR2 and mGluR3. Values in parentheses indicate number of cells tested. $*P = 0.0097$ (unpaired two-tailed *t*-test). **d**, smFRET histograms for mGluR3 show occupancy of the low FRET state that is abolished by the removal of Ca^{2+} or introduction of the Ser152Asp mutation. **e**, Representative smFRET traces for mGluR3 in the absence of Ca^{2+} with either 0 (top) or saturating (bottom) glutamate. **f**, Cross-correlation plots fit to a single exponential function for mGluR3. **g**, **h**, Dwell time of the active state for mGluR3 in the presence of glutamate (100 nM) or Ca^{2+} (2 mM) compared to mGluR2 (4 μM glutamate) (unpaired two-tailed *t*-test, $*P = 0.00055$). Error bars are s.e.m.

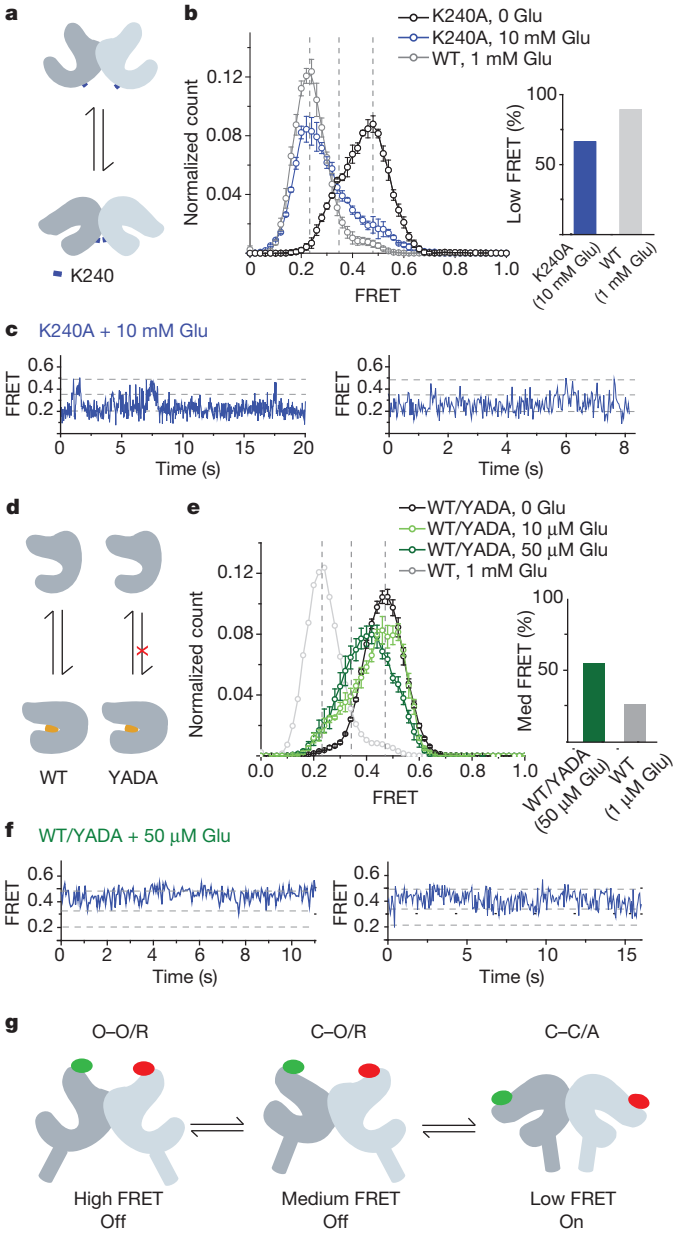

Figure 4 | A three-state model of mGluR activation. **a**, **b**, Mutation of residue Lys240 at the lower lobe LBD dimer interface (blue marker) (**a**) decreases occupancy of the low FRET state at saturating (10 mM) glutamate (**b**). WT, wild type. **c**, Representative smFRET traces for Lys240Ala in the presence of glutamate show transitions out of the low FRET state. **d**, **e**, Heterodimers of wild-type mGluR2 and the glutamate-insensitive mGluR2 (YADA) mutant (**d**) show enhanced occupancy of the medium FRET state (**e**). **f**, Representative smFRET traces for WT/YADA heterodimers show transitions between the high and medium FRET states with limited visits to the low FRET state. **g**, Three-state structural model of mGluRs based on intra-subunit (closed 'C' to open 'O') and inter-subunit (relaxed 'R' to active 'A') conformational changes. Error bars are s.e.m.

active conformation of mGluR3 is more stable than in mGluR2. Consistent with this, the time scale of donor and acceptor cross-correlation for mGluR3 in all conditions was much slower than for mGluR2 (Extended Data Fig. 9c). Overall, smFRET measurements revealed that mGluR3 transitions between the same three FRET states as mGluR2. However, unlike mGluR2, mGluR3 is Ca^{2+}-sensitive and therefore basally active under physiological conditions.

Having observed three ligand-dependent FRET states in the LBDs of both mGluR2 and mGluR3, we sought to identify the underlying conformational rearrangements in the activation pathway. The available structures of mGluR LBDs have been characterized as either 'relaxed', with the lower lobes of the LBD far apart, or 'active', with the lower lobes of the LBD closer to one other (Fig. 4a and Extended Data Fig. 10a). We proposed that electrostatic interactions between charged residues in the lower lobe, including a conserved lysine (Lys240 in mGluR2), stabilize the active conformation. Indeed, neutralizing Lys240 (Lys240Ala) decreased the apparent affinity for glutamate in both ensemble FRET and GIRK activation assays in cells (Extended Data Fig. 10b). In the smFRET assay, even at saturating glutamate concentrations (10 mM), this mutant populated the low FRET state less than wild-type mGluR2 (Fig. 4b). Single-molecule trajectories showed frequent transitions out of the low FRET state in saturating glutamate (Fig. 4c and Extended Data Fig. 10c), consistent with destabilization of the active state. These results support the idea that the lower lobes of mGluR2 come into close proximity in the active state and help to stabilize it.

We next investigated the conformations corresponding to the high (0.45) and medium (0.35) FRET states. Considering the comparatively small distance change between high and medium FRET states (~4 Å) compared to medium and low FRET states (~8 Å), and the observation that the medium FRET state seems to be inactive, we proposed that the medium state corresponds to a relaxed conformation in which only one LBD has closed. If this is true, an mGluR2 heterodimer composed of a wild-type subunit and a YADA subunit (wild-type/YADA) is expected to bind glutamate only in the wild-type LBD, and therefore populate the middle FRET state more than the wild-type homodimer. smFRET analysis showed that at near-saturating concentrations for the wild-type subunit, wild-type/YADA had an ~55% occupancy of the medium FRET state, whereas wild-type/wild-type had a maximal medium FRET occupancy of ~25% (Fig. 4d, e and Extended Data Fig. 10d–f). Unlike the mono-phasic concentration-dependence of occupancy of the low FRET state seen in wild-type mGluR2 (Fig. 1f), wild-type/YADA showed a biphasic distribution (Extended Data Fig. 10g), resembling the previously reported dose-response of effector activation by the wild-type/YADA heterodimer of mGluR5 (ref. 19), and supporting the assignment of the low smFRET conformation to the active state. smFRET traces at 50 µM glutamate showed numerous transitions between the high and medium FRET states with rare and brief visits to the low FRET state (Fig. 4f and Extended Data Fig. 10h), consistent with the activity of this heterodimer, and possibly due to occasional binding of glutamate to the YADA subunit or spontaneous closure of the YADA subunit in the absence of glutamate.

Our kinetic, mutational and functional analyses indicate that mGluR2 and mGluR3 undergo ligand-dependent fluctuations between three conformations: a resting and inactive O–O/R conformation, an active C–C/A conformation and an intermediate inactive short-lived C–O/R conformation (in which 'C' denotes 'closed', 'O' denotes 'open', 'R' denotes 'relaxed' and 'A' denotes 'active') (Fig. 4g). The relative instability of the intermediate conformation may explain why crystal structures have not been obtained in the C–O/R state.

Electrostatic interactions at the lower lobe LBD interface stabilize the active state, suggesting that mGluR activation requires closure of both LBDs followed by rearrangement of the dimer interface (Fig. 4g) and consistent with findings that activation requires downstream reorientation at the inter-subunit interfaces between cysteine-rich domains and TMDs[23–26]. We observed occupancy times of tens of milliseconds to seconds—on the timescale of G protein signalling[27]—for both the O–O/R and C–C/A conformations. This is longer than the sub-millisecond fluctuations seen in isolated LBDs using diffusion-based FRET[28], suggesting that the TMD of the intact receptor stabilizes the LBDs in the R and A states, giving the receptors a wide dynamic range of activity. Our findings suggest that the fractional occupancy of the C–C/A conformation determines agonist efficacy, consistent with isolated LBD single-molecule spectroscopy[28] and crystal structures, in

which the degree of closure is similar for full and partial agonists[18,19,29]. Finally, we revealed kinetic differences between mGluR2 and mGluR3 and found that mGluR3 has a more stable active state and is activated by physiological concentrations of external Ca^{2+}, resulting in considerable basal G-protein signalling in cells. Our study provides a framework for investigating the activation mechanisms of other bi-lobed, clamshell LBDs, such as in the $GABA_B$ receptor and ionotropic neurotransmitter receptors.

Online Content Methods, along with any additional Extended Data display items and Source Data, are available in the online version of the paper; references unique to these sections appear only in the online paper.

Received 3 December 2014; accepted 19 June 2015.
Published online 10 August 2015.

1. Rasmussen, S. G. *et al.* Crystal structure of the β_2 adrenergic receptor-Gs protein complex. *Nature* **477,** 549–555 (2011).
2. Katritch, V., Cherezov, V. & Stevens, R. C. Structure-function of the G protein-coupled receptor superfamily. *Annu. Rev. Pharmacol. Toxicol.* **53,** 531–556 (2013).
3. Conn, P. J. & Pin, J. P. Pharmacology and functions of metabotropic glutamate receptors. *Annu. Rev. Pharmacol. Toxicol.* **37,** 205–237 (1997).
4. Niswender, C. M. & Conn, P. J. Metabotropic glutamate receptors: physiology, pharmacology, and disease. *Annu. Rev. Pharmacol. Toxicol.* **50,** 295–322 (2010).
5. Kniazeff, J. *et al.* Locking the dimeric $GABA_B$ G-protein-coupled receptor in its active state. *J. Neurosci.* **24,** 370–377 (2004).
6. Kumar, J. & Mayer, M. L. Functional insights from glutamate receptor ion channel structures. *Annu. Rev. Physiol.* **75,** 313–337 (2013).
7. Kunishima, N. *et al.* Structural basis of glutamate recognition by a dimeric metabotropic glutamate receptor. *Nature* **407,** 971–977 (2000).
8. Tsuchiya, D., Kunishima, N., Kamiya, N., Jingami, H. & Morikawa, K. Structural views of the ligand-binding cores of a metabotropic glutamate receptor complexed with an antagonist and both glutamate and Gd^{3+}. *Proc. Natl Acad. Sci. USA* **99,** 2660–2665 (2002).
9. Roy, R., Hohng, S. & Ha, T. A practical guide to single-molecule FRET. *Nature Methods* **5,** 507–516 (2008).
10. Zhao, Y. *et al.* Single-molecule dynamics of gating in a neurotransmitter transporter homologue. *Nature* **465,** 188–193 (2010).
11. Bockenhauer, S., Furstenberg, A., Yao, X. J., Kobilka, B. K. & Moerner, W. E. Conformational dynamics of single G protein-coupled receptors in solution. *J. Phys. Chem. B* **115,** 13328–13338 (2011).
12. Morrison, E. A. *et al.* Antiparallel EmrE exports drugs by exchanging between asymmetric structures. *Nature* **481,** 45–50 (2011).
13. Keppler, A. *et al.* A general method for the covalent labeling of fusion proteins with small molecules *in vivo*. *Nature Biotechnol.* **21,** 86–89 (2003).
14. Doumazane, E. *et al.* A new approach to analyze cell surface protein complexes reveals specific heterodimeric metabotropic glutamate receptors. *FASEB J.* **25,** 66–77 (2011).
15. Doumazane, E. *et al.* Illuminating the activation mechanisms and allosteric properties of metabotropic glutamate receptors. *Proc. Natl Acad. Sci. USA* **110,** E1416–E1425 (2013).
16. Jain, A. *et al.* Probing cellular protein complexes using single-molecule pull-down. *Nature* **473,** 484–488 (2011).
17. Kniazeff, J. *et al.* Closed state of both binding domains of homodimeric mGlu receptors is required for full activity. *Nature Struct. Mol. Biol.* **11,** 706–713 (2004).
18. Jin, R., Banke, T. G., Mayer, M. L., Traynelis, S. F. & Gouaux, E. Structural basis for partial agonist action at ionotropic glutamate receptors. *Nature Neurosci.* **6,** 803–810 (2003).
19. Yamashita, T., Kai, T., Terakita, A. & Shichida, Y. A novel constitutively active mutation in the second cytoplasmic loop of metabotropic glutamate receptor. *J. Neurochem.* **91,** 484–492 (2004).
20. Yanagawa, M., Yamashita, T. & Shichida, Y. Activation switch in the transmembrane domain of metabotropic glutamate receptor. *Mol. Pharmacol.* **76,** 201–207 (2009).
21. Kubo, Y., Miyashita, T. & Murata, Y. Structural basis for a Ca^{2+}-sensing function of the metabotropic glutamate receptors. *Science* **279,** 1722–1725 (1998).
22. Nash, M. S., Saunders, R., Young, K. W., Challiss, R. A. & Nahorski, S. R. Reassessment of the Ca^{2+} sensing property of a type I metabotropic glutamate receptor by simultaneous measurement of inositol 1,4,5-trisphosphate and Ca^{2+} in single cells. *J. Biol. Chem.* **276,** 19286–19293 (2001).
23. Tateyama, M., Abe, H., Nakata, H., Saito, O. & Kubo, Y. Ligand-induced rearrangement of the dimeric metabotropic glutamate receptor 1alpha. *Nature Struct. Mol. Biol.* **11,** 637–642 (2004).
24. Huang, S. *et al.* Interdomain movements in metabotropic glutamate receptor activation. *Proc. Natl Acad. Sci. USA* **108,** 15480–15485 (2011).
25. Hlavackova, V. *et al.* Sequential inter- and intrasubunit rearrangements during activation of dimeric metabotropic glutamate receptor 1. *Sci. Signal.* **5,** ra59 (2012).
26. Xue, L. *et al.* Major ligand-induced rearrangement of the heptahelical domain interface in a GPCR dimer. *Nature Chem. Biol.* **11,** 134–140 (2015).
27. Lohse, M. J., Maiellaro, I. & Calebiro, D. Kinetics and mechanism of G protein-coupled receptor activation. *Curr. Opin. Cell Biol.* **27,** 87–93 (2014).
28. Olofsson, L. *et al.* Fine tuning of sub-millisecond conformational dynamics controls metabotropic glutamate receptors agonist efficacy. *Nature Commun.* **5,** 5206 (2014).
29. Muto, T., Tsuchiya, D., Morikawa, K. & Jingami, H. Structures of the extracellular regions of the group II/III metabotropic glutamate receptors. *Proc. Natl Acad. Sci. USA* **104,** 3759–3764 (2007).

Acknowledgements We thank Z. Fu and H. Okada for technical assistance, J. P. Pin for generously providing the SNAP- and CLIP-tagged mGluRs and advice on their properties, and J. P. Pin, E. Margeat, P. Rondard, A. Jain, A. Reiner and members of the Isacoff laboratory for discussions. Funding was provided by the National Institutes of Health Nanomedicine Development Center for the Optical Control of Biological Function (2PN2EY018241) and the National Science Foundation (EAGER: IOS-1451027). R.V. is a Merck fellow of the Life Science Research Foundation.

Author Contributions R.V., J.L. and E.Y.I. designed the research. R.V. set up, performed and analysed single-molecule FRET experiments. J.L. performed and analysed ensemble FRET and electrophysiology experiments and contributed to single-molecule FRET experiments. R.V., J.L. and E.IY. wrote the paper.

Author Information Reprints and permissions information is available at www.nature.com/reprints. The authors declare no competing financial interests. Readers are welcome to comment on the online version of the paper. Correspondence and requests for materials should be addressed to E.Y.I. (ehud@berkeley.edu).